

RESEARCH ARTICLE

Electronic Characterization of Au/DNA/ITO Metal-Semiconductor-Metal Diode and Its Application as a Radiation Sensor

Hassan Maktuff Jaber Al-Ta'ii^{1,3*}, Vengadesh Periasamy^{1*}, Yusoff Mohd Amin²

1 Low Dimensional Materials Research Centre (LDMRC), Department of Physics, Faculty of Science, University of Malaya, 50603 Kuala Lumpur, Malaysia, **2** Department of Physics, Faculty of Science, University of Malaya, 50603 Kuala Lumpur, Malaysia, **3** Department of Physics, Faculty of Science, University of Al-Muthana, Al-Muthana 66001, Iraq

* hassankirkukly@gmail.com (HMJA-T); vengadeshp@um.edu.my (VP)



Abstract

Deoxyribonucleic acid or DNA molecules expressed as double-stranded (DSS) negatively charged polymer plays a significant role in electronic states of metal/silicon semiconductor structures. Electrical parameters of an Au/DNA/ITO device prepared using self-assembly method was studied by using current–voltage (I-V) characteristic measurements under alpha bombardment at room temperature. The results were analyzed using conventional thermionic emission model, Cheung and Cheung's method and Norde's technique to estimate the barrier height, ideality factor, series resistance and Richardson constant of the Au/DNA/ITO structure. Besides demonstrating a strongly rectifying (diode) characteristic, it was also observed that orderly fluctuations occur in various electrical parameters of the Schottky structure. Increasing alpha radiation effectively influences the series resistance, while the barrier height, ideality factor and interface state density parameters respond linearly. Barrier height determined from I–V measurements were calculated at 0.7284 eV for non-radiated, increasing to about 0.7883 eV in 0.036 Gy showing an increase for all doses. We also demonstrate the hypersensitivity phenomena effect by studying the relationship between the series resistance for the three methods, the ideality factor and low-dose radiation. Based on the results, sensitive alpha particle detectors can be realized using Au/DNA/ITO Schottky junction sensor.

OPEN ACCESS

Citation: Al-Ta'ii HMJ, Periasamy V, Amin YM (2016) Electronic Characterization of Au/DNA/ITO Metal-Semiconductor-Metal Diode and Its Application as a Radiation Sensor. PLoS ONE 11(1): e0145423. doi:10.1371/journal.pone.0145423

Editor: Goran Karapetrov, Drexel University, UNITED STATES

Received: August 21, 2015

Accepted: December 3, 2015

Published: January 22, 2016

Copyright: © 2016 Al-Ta'ii et al. This is an open access article distributed under the terms of the [Creative Commons Attribution License](https://creativecommons.org/licenses/by/4.0/), which permits unrestricted use, distribution, and reproduction in any medium, provided the original author and source are credited.

Data Availability Statement: All relevant data are within the paper and its Supporting Information files.

Funding: This work was supported by Fundamental Research Grant Scheme, FRGS (FP004-2013A), University of Malaya Postgraduate Research Fund, PPP (PG202-2014B) and University of Malaya Research Grant, UMRG (RG321-15AFR).

Competing Interests: The authors have declared that no competing interests exist.

Introduction

Deoxyribonucleic acid (DNA) has many advantages, mainly due to its vast accessibility, size manipulation capabilities and natural self-assembly properties [1]. However, the right genomic sequence, structure, environment and other properties are the pre-requisites necessary for generating optimized optical and electronic properties towards various stimuli [2, 3] leading to possible control of the properties [4]. For example, DNA molecules expressed as double-stranded (DSS) negatively charged phosphate group polymer and aromatic bases plays an

important role in electronic states of metal/silicon semiconductor structures [1, 5]. Various other groups have also investigated and measured optimized DNA response towards magnetic field [6, 7], temperature [8], radiation [9, 10] and others [11].

Radiation has the ability to modify the flexibility of DNA. When irradiated using gamma rays and neutrons (non-ionizing radiation) the dynamics of DNA macromolecules [12] changes its configuration when involved in environmental interactions with other components of the living cells [13]. Electronic features of a Schottky diode is described by its barrier height, ideality factor and series resistance parameters. These features are in turn affected by factors like temperature [8, 14], interface [15], humidity [16, 17], and radiation [18, 19]. Whenever any radiation passes through a semiconductor device, different effects are observed depending on the range of energy of the particle (proton, alpha, neutron and both types of beta) and rays, such as gamma radiation [20]. These include defects such as vacancies, defect clusters, dislocation loops near the surface and adjustment of band gaps [21].

Electrical properties of DNA molecules can be understood by studying the electrical conduction mechanism. Three different mechanisms have been proposed; thermionic emission [22], tunneling and hopping [23, 24]. Recently, researchers studying the magnetic effect on DNA observed increase in the potential barrier between DNA and two gold (Au) wires as electrodes. Based on measurements of current-voltage (I-V) curve and Schottky's rule, they suggested potential of the metal-DNA-metal (MDM) structures for utilization as sensitive magnetic sensors [6]. Güllü *et al* meanwhile used solution-processing method to fabricate a DNA organic-on-inorganic Schottky device. Based on the electrical properties of this device, effects of DNA interlayer on conventional metal/semiconductor [3] were also evaluated. In another work, Güllü *et al* in 2011 observed the effect of temperature on the current transport characteristics of Al/DNA/p-Si Schottky diodes in the range of 200–300 K [8]. Bellido *et al* analyzed I-V-temperature characteristics and observed current passing through a triangular DNA origami rely on the temperature when surrounded between two platinum electrodes [23]. Kulkarni *et al* recently discussed the feasibility of a DNA thin film as a radiation sensing material and considered it for sensing radiation based on reflected intensity variations of the exposed DNA thin film and biomolecules [9]. Thomas *et al* demonstrated that the reliability of the connection was improved when organic semiconductor buffer film was inserted between two metal electrodes and the DNA as gold/DNA/Pt. DNA could be destroyed by a direct metal evaporation process, which retards current production. According to Hassan *et al*, Ha *et al*, and Güllü *et al*, the electronic properties of DNA such as the I-V profiles are generally influenced by the contact, bulk (DNA channel) and intermolecular features under environmental conditions such as humidity effect and irradiation. It could also be assumed that the majority of response is initiated by the Schottky metal (Au) -semiconductor (DNA) contact. [19, 25, 26]. Conductivity sharply declines because of the long exposure in dry nitrogen or in vacuum. As such, it could be concluded that ion hydration shell and water molecules of the DNA plays a major part, with its conductivity evaluated at about 10^{-6} – 10^{-5} S·cm⁻¹ per DNA molecule [27]. Okahata *et al* meanwhile measured the conductivity of the DNA placed on electrode comb to be 5.6×10^{-5} and 10^{-9} S cm⁻¹ for current flow parallel and vertical to the aligned DNA strands, respectively [28]. The conductance was increased between two to five times when doping the metal ion onto the DNA crystals for some samples as such as with 4 mM of [Cu²⁺], 1.5 mM of [Ni²⁺], 1 mM of [Zn²⁺] and 0.6 mM of [Co²⁺] [29]. Recently, Dugasani *et al* observed that the resistivity tendency and Hall mobility declined when the ion concentration was raised while reaching the saturation concentration (C_s) of each metal ion, thereby increasing the ion concentration. Also, they numerically discovered that the metal-DNA lattice behaved as a semiconductor with metal ions through the Hall parameters [30]. In this current work, we report the study of the current transport characteristics of Au/DNA/ITO Schottky diodes exposed to

alpha radiation between 0–0.24 Gy. The current transport mechanism in these diodes was described using the features of forward I–V graphs. Additionally, we show the difference of the ideality factors, n , and the barrier heights, Φ at different exposure dose. The results obtained based on three methods (conventional, Cheung and Cheung's and Norde methods) suggests the possibility of applying the Schottky junction as a sensitive sensor element to detect alpha particles.

Experimental Section

2.1. Preparation of DNA solution

A simple preparation procedure of mushroom DNA extracted from colonies of fruiting bodies was used for Polymerase Chain Reaction (PCR) amplification. The DNA Kit was purchased from (OMEGA Bio-tek E.Z.N.A.). The procedure starts with the collection of minute quantities of mycelium (0.1–1.0 g) from a colony of the fruiting body (Stipe) of a mushroom species using a sterilized tweezers. Standard procedures according to [31] were further employed to yield pure DNA samples prior to the PCR process. The DNA of all samples was amplified by PCR (PTC-100TM, MJ Research Inc., U.S.A.) using universal primers ITS1 forward (5'-TCC GTA GGTGAACCTGCGG-3') and ITS4 reverse (5'-TCCTCCGCTT ATT GATATGC-3'). Amplification reactions were performed in a total volume of 50 μ l containing 10x PCR buffer 4.0 μ l, dNTP mix 2.5 μ l, 2.5 μ l of each primer, 1.0 μ l of Taq polymerase (Cosmo, Korea), 4.0 μ l of genomic template DNA, and 26.0 μ l of sterilized distilled water. PCR amplification was carried out in 30 cycles at 94°C for 30 minutes and denatured at 50°C for 60 minutes followed by annealing at 72°C for an extension of 1 minute. Initial denaturing at 95°C was extended to 5 minutes and the final extension was at 72°C for 5 minutes [32, 33].

2.2. ITO cleaning procedures

ITO slides of width 1.1 mm purchased from KINTEC, Hong Kong had a layer thickness of 100 nm with a dimension of 2 cm x 2 cm and 377.0 Ω /sq and about 10^4 S/cm of sheet resistance and conductivity, respectively. Thickness of the Au wire electrodes used was (0.50 \pm 0.05) mm and purity 99.999% (Sigma Aldrich, USA). Prior to diode fabrication, the ITO substrates were cleaned thoroughly. In order to remove any oxides, the ITO slides were rinsed with soap in an ultrasonic bath for 10–15 minutes. The slides were washed using deionized water and dipped in acetone and iso-propyl alcohol (isopropanol, C₃H₈O) for 5 minutes each followed by final rinsing using deionized water. The chemicals were purchased from R&M chemicals (Essex, UK). Finally, the slides were dried using nitrogen gas to remove water and any other residues.

2.3. DNA film deposition

DNA films were prepared by placing 10.0 μ l of DNA solution of concentration of 1.80 ng/ μ l onto clean ITO glass substrates. The prepared DNA films were air-dried for 24 hours in a 1K clean room before irradiation. Sample irradiation by alpha particles was achieved using ²⁴¹Am with an activity of 150 nCurie and $t_{1/2}$ of 457 years for dose 0–0.24 Gy and the corresponding I–V profiles recorded. Fig 1 depicts the schematic diagram of the sensor fabricated for measuring the I–V characteristics (Keithley Electrometer, SMU236) and thickness of the DNA based on the Atomic Force Microscope (AFM) (Q-Scope Series, Ambios Technology, Germany) derived depth profiles of the DNA film. Width for non-irradiated and 0.012 and 0.024 Gy of radiation were 150, 7.5 and 5.5 nm, respectively, demonstrating a reduction in DNA layer thickness with increasing dose.

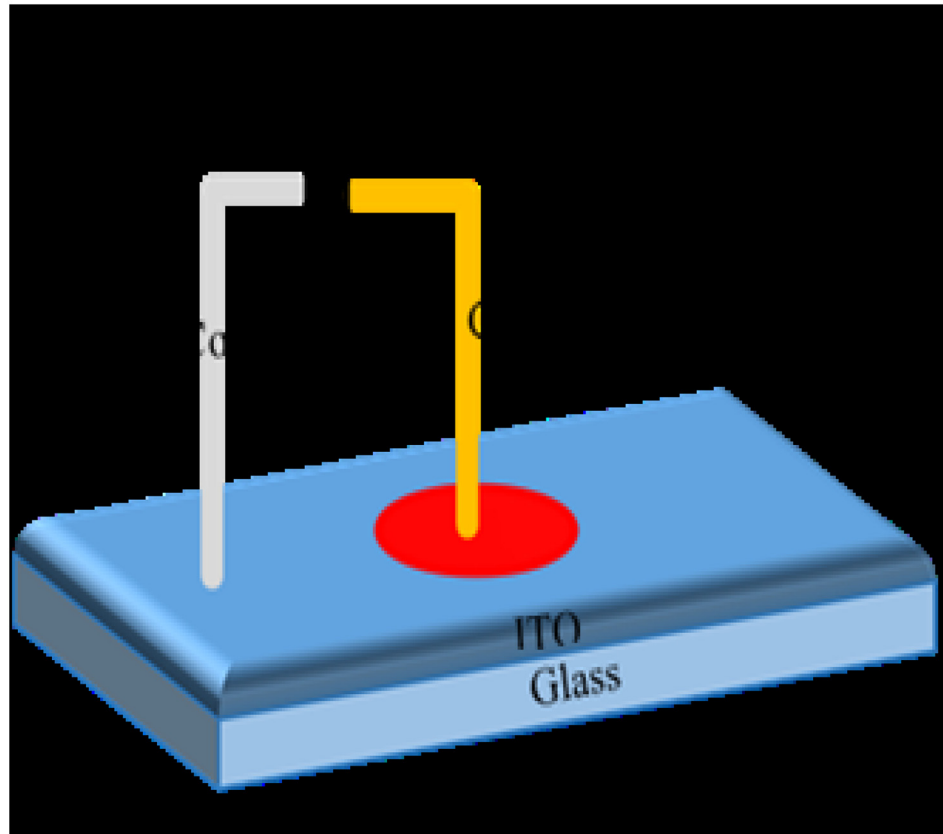


Fig 1. Cross-sectional view of Au/DNA/ITO Schottky diode.

doi:10.1371/journal.pone.0145423.g001

Results and Discussion

I-V characteristics of the Au/DNA/ITO (MS) Schottky structure at 300K (room temperature) are shown in Fig 2, described by the following relations [22, 34–38];

$$I = I_0 \exp\left(\frac{qV}{nKT}\right) \left[1 - \exp\left(\frac{-qV}{KT}\right) \right] \quad (1)$$

and

$$I_0 = AA^*T^2 \left(\frac{-q\Phi}{KT} \right) \quad (2)$$

where I_0 is the saturation density, V is the definite forward-bias voltage, A is the effective diode area, K is the Boltzmann constant, T is the absolute temperature, A^* is the Richardson constant for Au ($A^* = 134.95 \text{ Acm}^{-2}\text{K}^{-2}$) [39].

The barrier height was calculated using Eq (2). The value of reverse saturation current is obtained from forward bias semi log (I)-V for all cases. Value of ideality factor, n was calculated from the slope of the linear region of the forward bias $\ln(I)$ -V plot in Fig 3 by using the

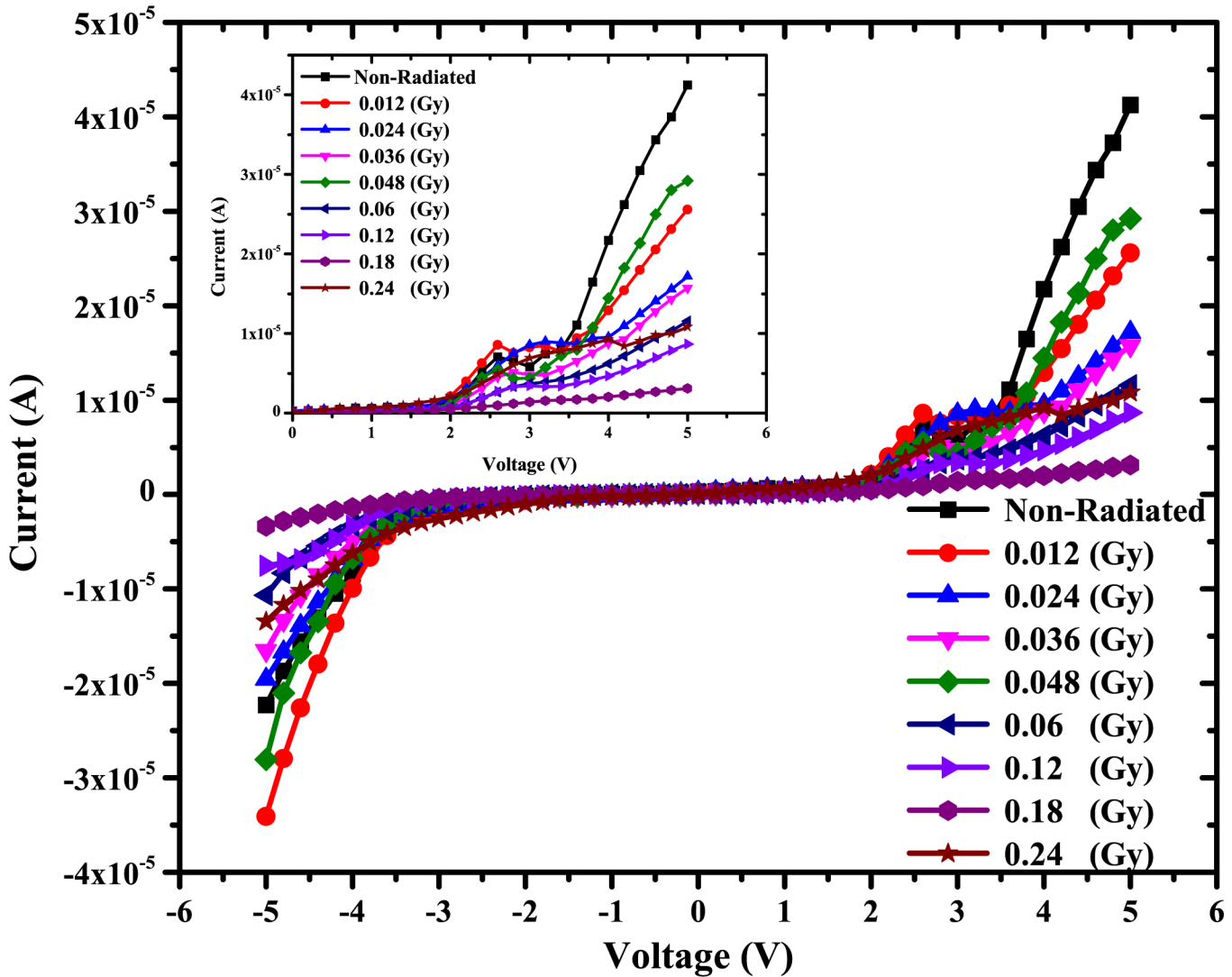


Fig 2. Current-voltage characteristics of Au/DNA/ITO Schottky structures.

doi:10.1371/journal.pone.0145423.g002

following relation [40];

$$n = \frac{q}{KT} \left(\frac{dV}{d \ln I} \right) \tag{3}$$

The values of the ideality factors are presented in Table 1. For an ideal Schottky barrier diode, n equals to 1. However, n has usually a value greater than unity. This value indicates that the effect of the series resistance in the linear region is important. Higher values of n may also be due to non-homogeneous thickness of organic film or light effect [36, 40]. The connection characteristics of DNA based diode rely on the thickness [41] and temperature [36, 42]. From

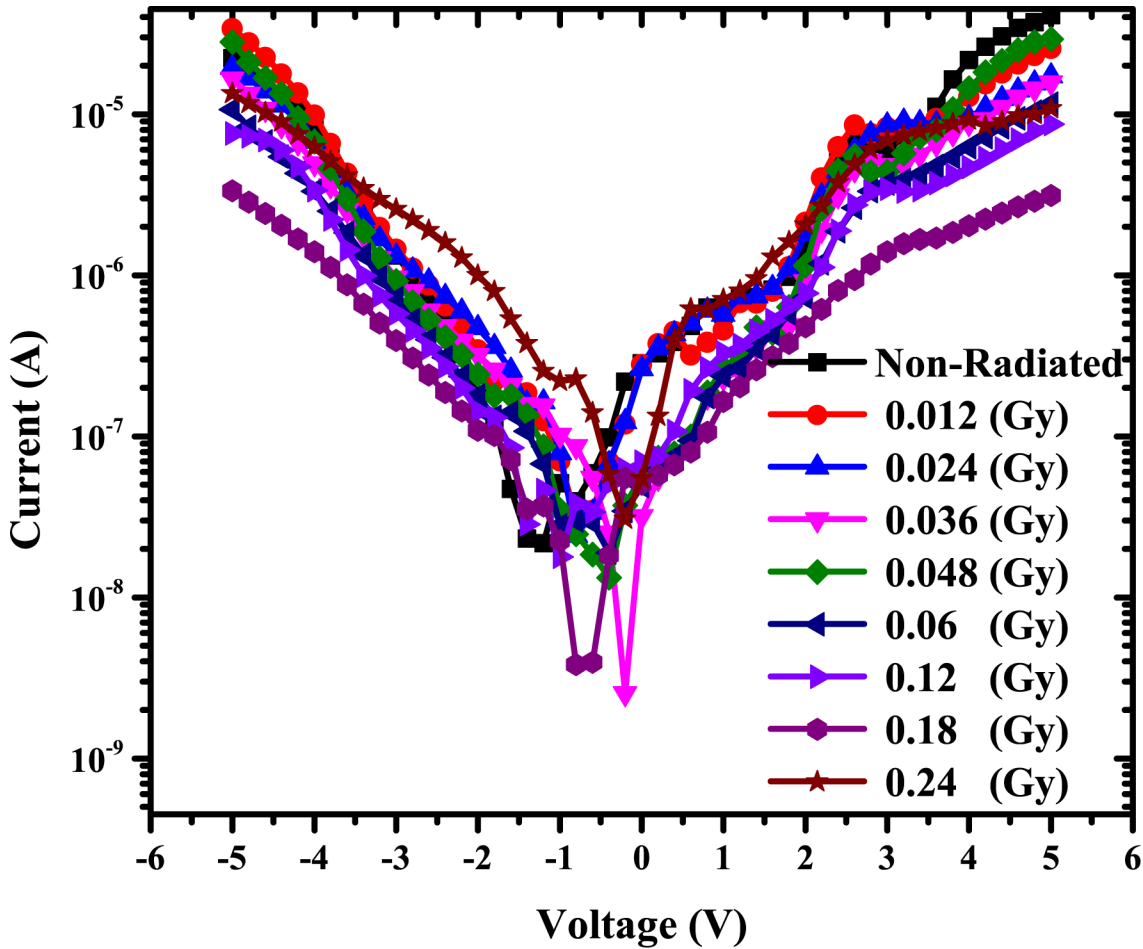


Fig 3. Forward and reverse bias I-V characteristics of the Au/DNA/ITO structures at room temperature.

doi:10.1371/journal.pone.0145423.g003

Table 1. Values of ideality factor, barrier height and series resistance measured. Uncertainties are shown for the Cheung and Cheung's Method obtained through curve fitting while no such values are shown for the other two models since it was calculated from the equations.

Dose (Gy)	Conventional Method			Cheung and Cheung's Model				Norde Method	
	n	Φ (eV)	R_s (M Ω)	n	R_s (M Ω)	Φ (eV)	R_s (M Ω)	Φ (eV)	R_s (M Ω)
Non-Radiated	1.35732	0.7284	0.120821	8.8803	0.0064±0.000157	0.6679	0.011±0.04468	0.7230	0.04244
0.012	1.37498	0.7600	0.171260	8.1081	0.0099±0.00113	0.685	0.028±0.00173	0.7201	0.04742
0.024	1.17205	0.7371	0.219648	7.3359	0.0120±0.000242	0.6653	0.043±0.002037	0.6732	0.06339
0.036	1.48465	0.7879	0.316129	6.9498	0.0180±0.00154	0.6895	0.096±0.00196	0.6568	0.11504
0.048	2.2488	0.7426	0.1711	3.4486	0.0154±0.001388	0.7172	0.066±0.00538	0.7188	0.04480
0.06	1.34893	0.7798	0.4329	2.2890	0.0392±0.002599	0.6926	0.078±0.0111	0.6962	0.11991
0.12	1.26426	0.7491	0.5768	1.6162	0.0534±0.003274	0.6819	0.148±0.0154	0.6963	0.12021
0.18	2.4033	0.7407	1.6	1.3019	0.128±0.005966	0.7007	1.012±0.0382	0.6744	0.24370
0.24	2.35403	0.7670	0.4333	1.4324	0.0356±0.001425	0.6794	0.24±0.0143	0.7142	0.05281

n = Ideality factor, Φ (eV) = Barrier height, R_s = Series resistance.

doi:10.1371/journal.pone.0145423.t001

Eq (2), the barrier height, Φ can be derived and shown by;

$$\Phi = \frac{KT}{q} \ln \left(\frac{AA^*T^2}{I_0} \right) \tag{4}$$

From Fig 3, the deep valley demonstrates non-zero current at 0 V for the samples with an offset-shift in the negative direction up to 0.2 and 0.8 V for the 0.036 and 0.18 Gy, respectively. It might be attributed to the alpha particle charge or dose (storage, trapping, and de-trapping of the charge carriers) agreeing with Dugasani *et al* [30] and with Reddy *et al* in terms of the creation of reverse molecule charge interaction between DNA and the metal [43].

Using Eqs (3) and (4), the values of barrier height (Φ_b) and the ideality factor (n) of the gold/DNA/ITO Schottky diode were obtained. The barrier height describes the potential barrier at the interface of the DNA and gold wire. Φ_b will limit the flow of charge carriers in the device. The highest values of Φ_b were related to non-uniform junctions at the interface. In addition, Φ_b and n rely on the interfacial layer thickness, the interface state density and series resistance [44, 45]. The values of series resistance is calculated from the junction resistance from

$R_s = \frac{\partial V}{\partial I}$ from the I-V properties of the diode. The resistance R_s versus voltage of the

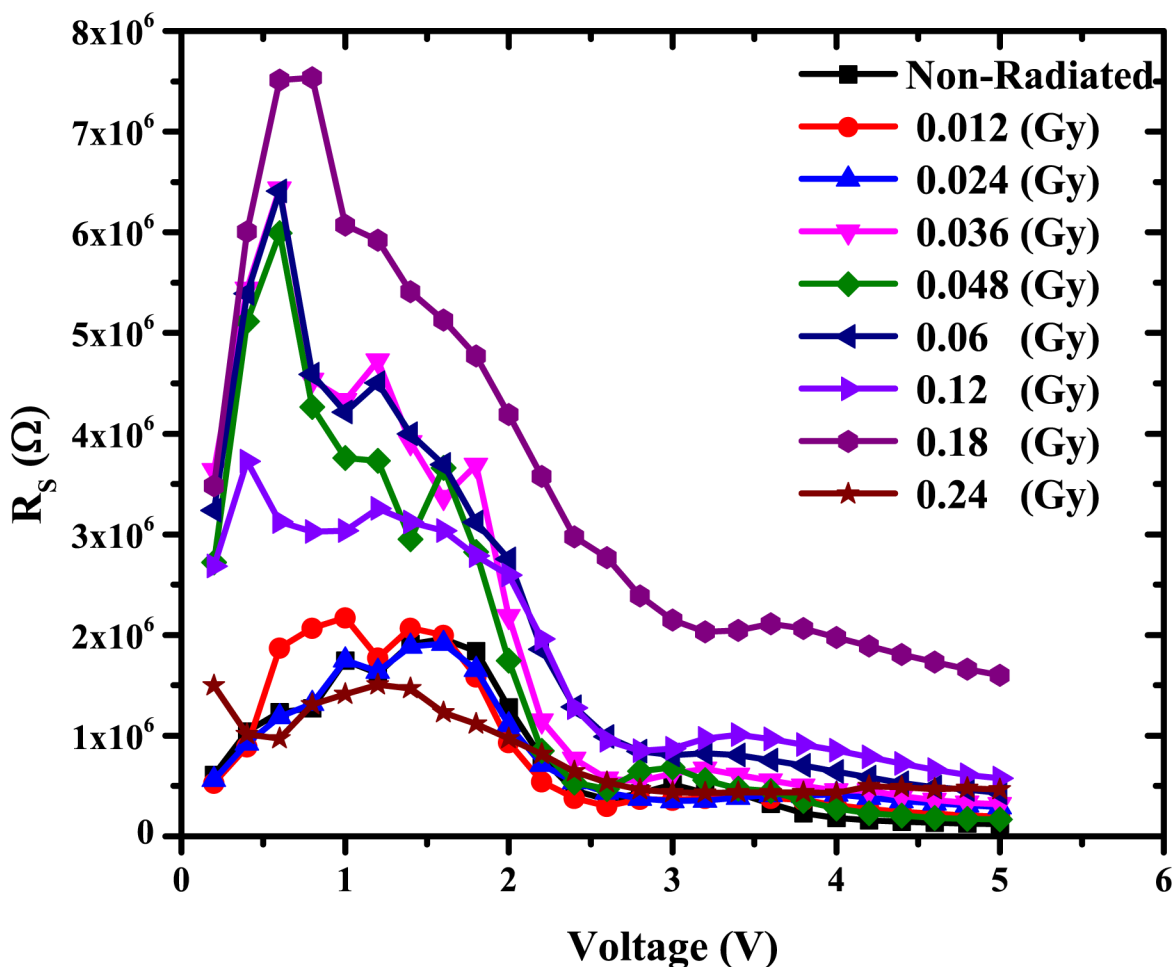


Fig 4. The relation between the series resistance versus voltage as calculated using the conventional method.

doi:10.1371/journal.pone.0145423.g004

surface-type (ITO/DNA/Au) Schottky diode is demonstrated in Fig 4. From the figure, it can be seen that at low voltages ($\leq 2.0V$), R_s values become the lowest for all the doses except for 0.18, 0.6, 0.048 and 0.036 Gy. However, above 2.0 V, the R_s values become insignificant for the latter sample. The highest R_s value occurs in the 0.18 Gy sample followed by 0.12 and 0.06 Gy.

The second method used in this study is the Cheung and Cheung’s model, which also considers the three parameters; series resistance, the barrier height and the ideality factor. Cheung and Cheung’s formula can be written as follows;

$$\frac{dV}{d\ln I} = IR_s + n\frac{KT}{q} \tag{5}$$

$$H(I) = V - \left(\frac{KT}{q}\right)\ln\left(\frac{I}{AA^*T^2}\right) \tag{6}$$

therefore

$$H(I) = IR_s + n\Phi_b \tag{7}$$

Fig 5(A) and 5(B) shows the experimental $H(I)$ versus I and $dV/d(\ln I)$ versus I plots respectively at room temperature. The former graph demonstrates a straight line intercepting at y-axis equaling to $n\Phi_b$. Φ_b was obtained by substituting the n value from Eq 5 and the data of the downward curvature region in the forward bias I-V using Eq 7. The slope of this plot also limits R_s , which can be utilized to check the accuracy of Cheung and Cheung’s method. From $H(I)$ versus I , the Φ_b and R_s values were measured and presented in Table 1. Eq 5 gives a straight line for the data of the downward curvature region in the forward bias I-V properties. Fig 5(B) shows the plot of $dV/d(\ln I)$ versus I , from which the values of n and R_s were calculated

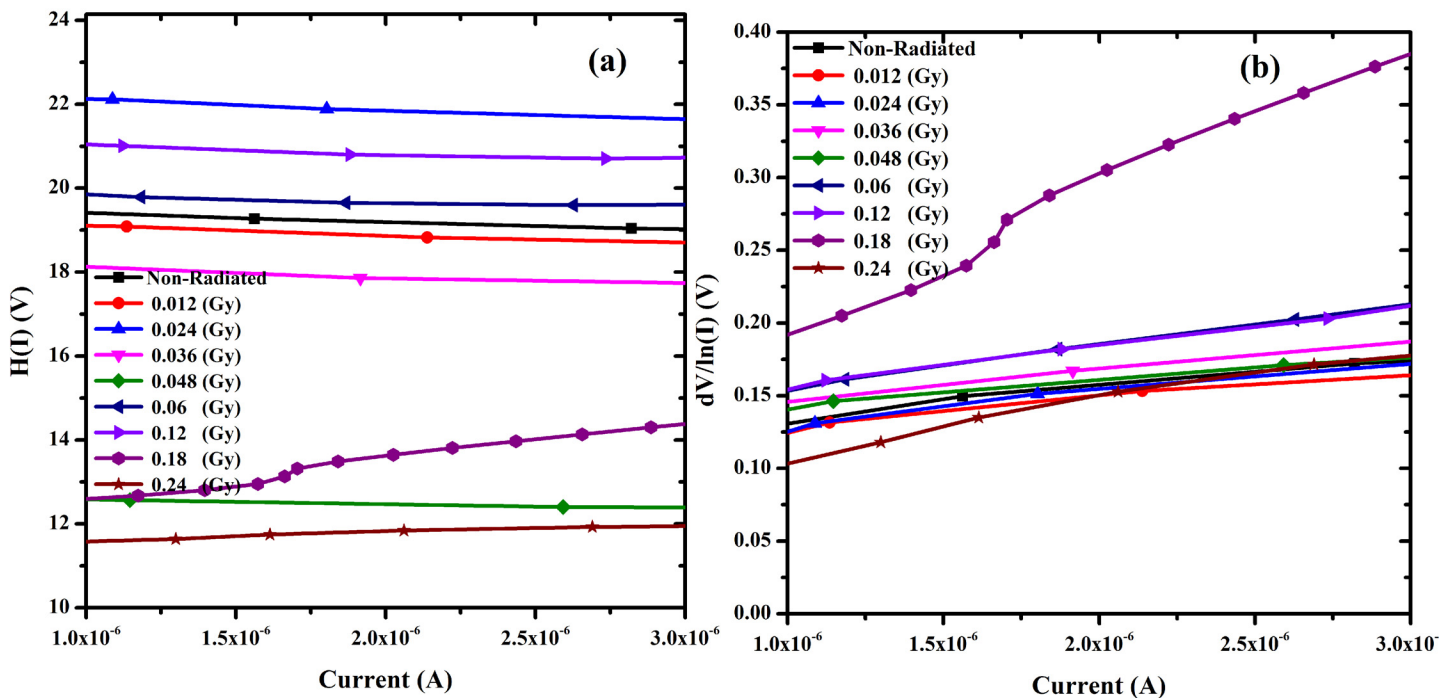


Fig 5. (a) $H(I)$ vs I and (b) $dV/d(\ln I)$ vs I characterization of Au/DNA/ITO Schottky junction diode.

doi:10.1371/journal.pone.0145423.g005

(Table 1). As can be seen from the table, the values of R_s obtained from $dV/d(\ln I)$ versus I and $H(I)$ versus I plots are in near agreement with each other.

Radiation dose however does play an important role in changing resistance values, thus the resistance increases gradually at low doses, which therefore makes the DNA seek self-protection. The real barrier height, (Φ_b) was taken from the low-voltage part of forward I-V graph while the series resistance from the straight-line region of Fig 5(A). Then the values of barrier height and the series resistance were obtained from Eq (7). All values from the conventional and the Cheung-Cheung's model are presented in Table 1 showing a general fluctuating trend with radiation dose.

Norde method meanwhile can be used as an alternative method to calculate values of the series resistance and barrier height [46]. The following function has been defined in modified Norde's method;

$$F(V) = \frac{V}{\gamma} - \frac{KT}{q} \ln\left(\frac{I}{AA^*T^2}\right) \tag{8}$$

The effective Schottky barrier height is therefore given by;

$$\Phi = F(V_{\min}) + \frac{V_{\min}}{\gamma} - \frac{KT}{q} \tag{9}$$

and

$$R_s = \frac{(\gamma - n)KT}{qI_o} \tag{10}$$

where $F(V_{\min})$ is the minimum point in the $F(V)$ versus V curve, V_{\min} and I_o are the corresponding voltage and current respectively. A plot of $F(V)$ versus V for Au/DNA/ITO Schottky structure at room temperature is as shown in Fig 6. From the plot $F(V)$ versus V , the values of Φ and R_s of the structure were determined and tabled (Table 1).

Plots of Φ , n and R_s with the radiation time shown in Figs 7(A) and 7(B) and 8 indicate the hypersensitivity phenomena of the DNA at low radiation dose. 0.4480 Gy.

The values were found to be the lowest using Cheung and Cheung's model compared to the other two methods with a general increase with the radiation dose. The values however fluctuate for barrier height in the case of Cheung and Cheung's model. Values of barrier height using Conventional method were closer to Norde's method, where the former have the lowest values.

From Fig 7(B), series resistance was found to increase with increasing radiation dose except in 0.05 Gy, probably due to the increasing number of alpha particle tracks (Fig 9). The thickness of the DNA film is as shown in Fig 9. Observations indicate general value of 1.24 μm with occasional dips of around 663 nm for the non-radiated sample. This increases to about 1.48 μm and 839 nm for the 0.012 Gy radiated sample. Further alpha radiation of 0.024 Gy reduces these values to 1.37 μm and 677 nm. This could be attributed to the alpha particles tracks, the hypersensitivity phenomena and due to the drop casting method used in this study.

At low doses, the R_s drop dramatically demonstrating the hypersensitivity phenomena of DNA Fig 8, which acts to protect itself. With further increase in time-dependent dosage, this phenomenon is similar to the relation between survival curve and dose [46–48]. By increasing the irradiation dose and conducting similar experiments for periods of 0, 2 and 4 min and the width for non-radiated and 0.012 and 0.024 Gy of irradiation dose are 150, 7.5 and 5.5 nm, respectively [10]. It was very clear in the conventional method that the Schottky barrier height on the other hand had an inverse proportionality relationship with the ideality factor as observed in Fig 8.

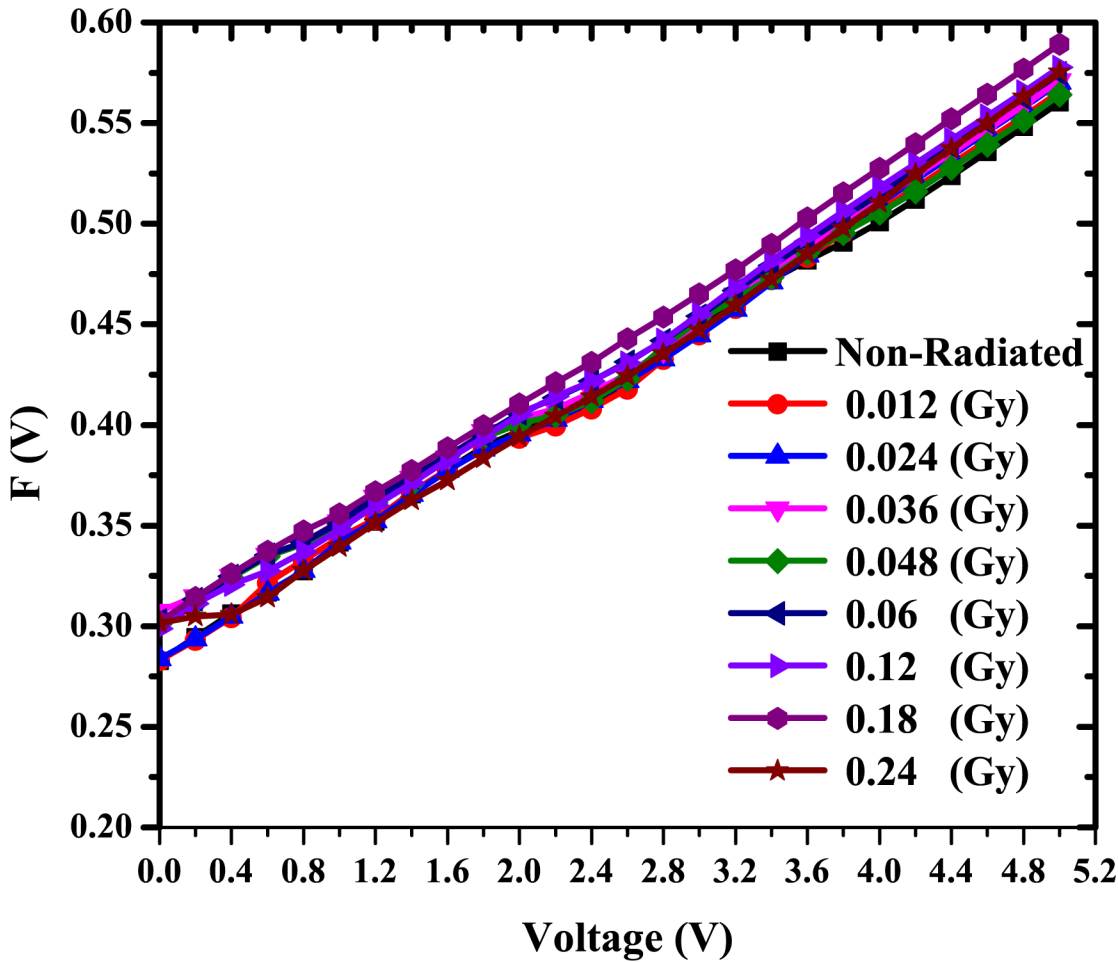


Fig 6. $F(V)$ versus applied voltage of the Au/DNA/ITO device Schottky diode.

doi:10.1371/journal.pone.0145423.g006

Richardson constant was determined from the I-V curve, and it rapid changes with dosage show Fig 10(A). The ionizing radiation process leads to energy sedimentation in the metal, denoted as thermal heat which changes the material characterization [20]. The work function of the metal/semiconductor junction changes, which affords sufficient energy for the charge carriers to get over the binding potential. Rising number of alpha particles tracks also leads to creation of higher number of holes, thereby increasing the effective mass. Since only a lower number of carriers are able to break through the potential barrier now, this would translate into a decrease in the current.

Due to the excitation of the material by ionizing radiation, such as by alpha particles, initially outputs an enormous number of excited atoms along its path, thereby increasing the number of electrons. However, continuous irradiation results in a decrease in the number of electrons as a result of collisions between the metal-DNA-metal (MDM) electrodes and the rise in resistance due to the number of traps in DNA preventing internal charge movement and hence increase the electrical resistance [49, 50]. The number of electrons also decreases through the collision between the metal-semiconductor-metal (MSM) electrodes. This results in the growth of the barrier heights as in Table 2, followed by a decline in the current. Fig 10(B) exhibits dual logarithmic plot of forward bias I-V features of the ITO/DNA/Au junction. The log (I)-log (V) graphs clearly shows the power law performance of the I-V curve.

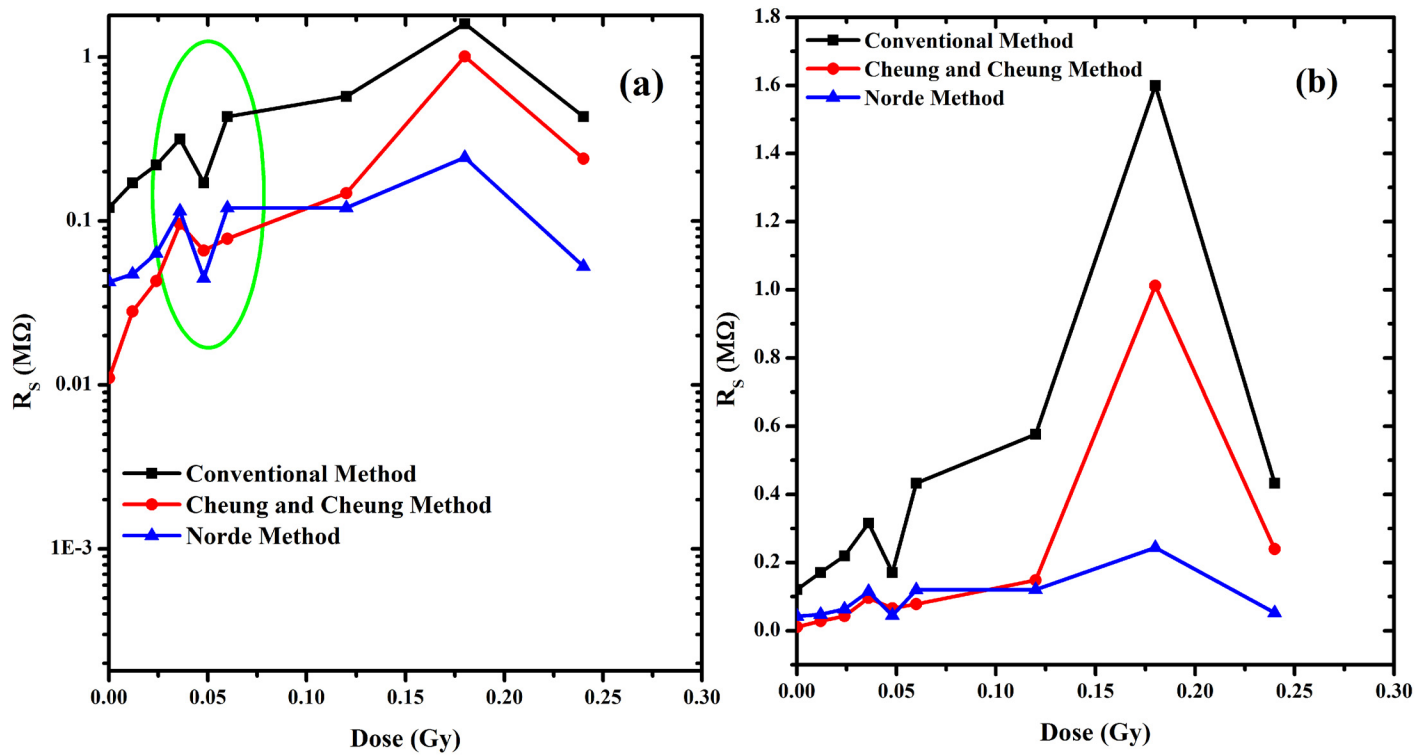


Fig 7. (a) Relation between series resistance and dose. (b) Relation between log series resistance and dose.

doi:10.1371/journal.pone.0145423.g007

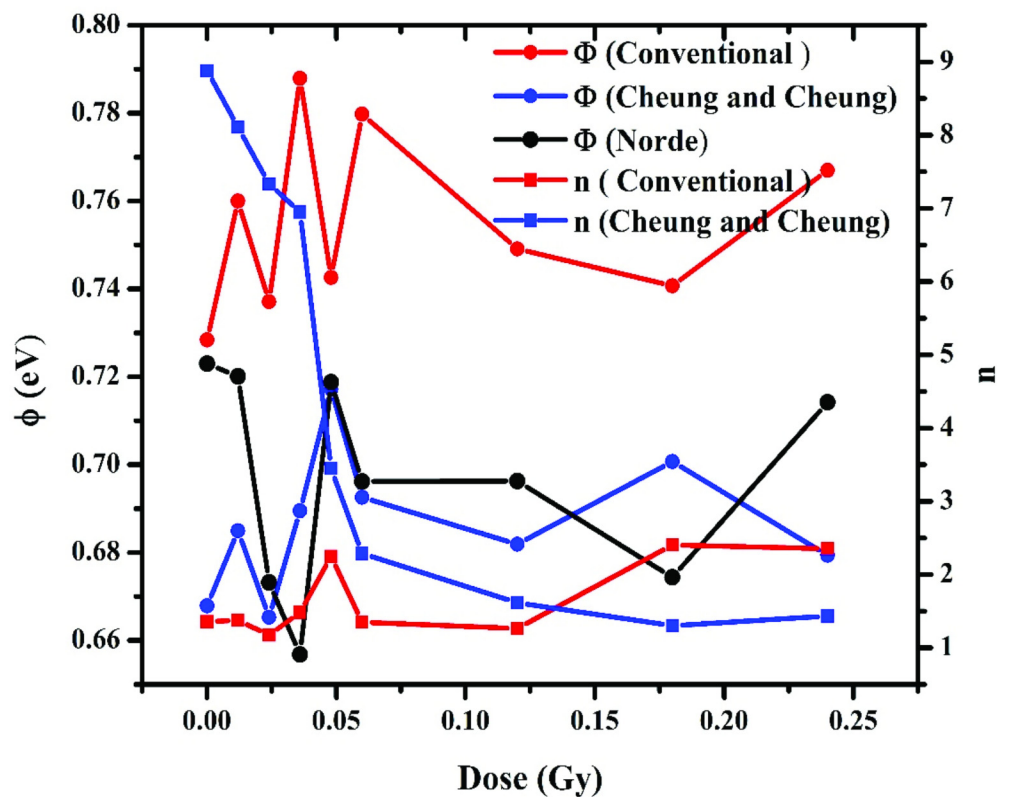


Fig 8. The relation between ideality factor and barrier height with radiation time.

doi:10.1371/journal.pone.0145423.g008

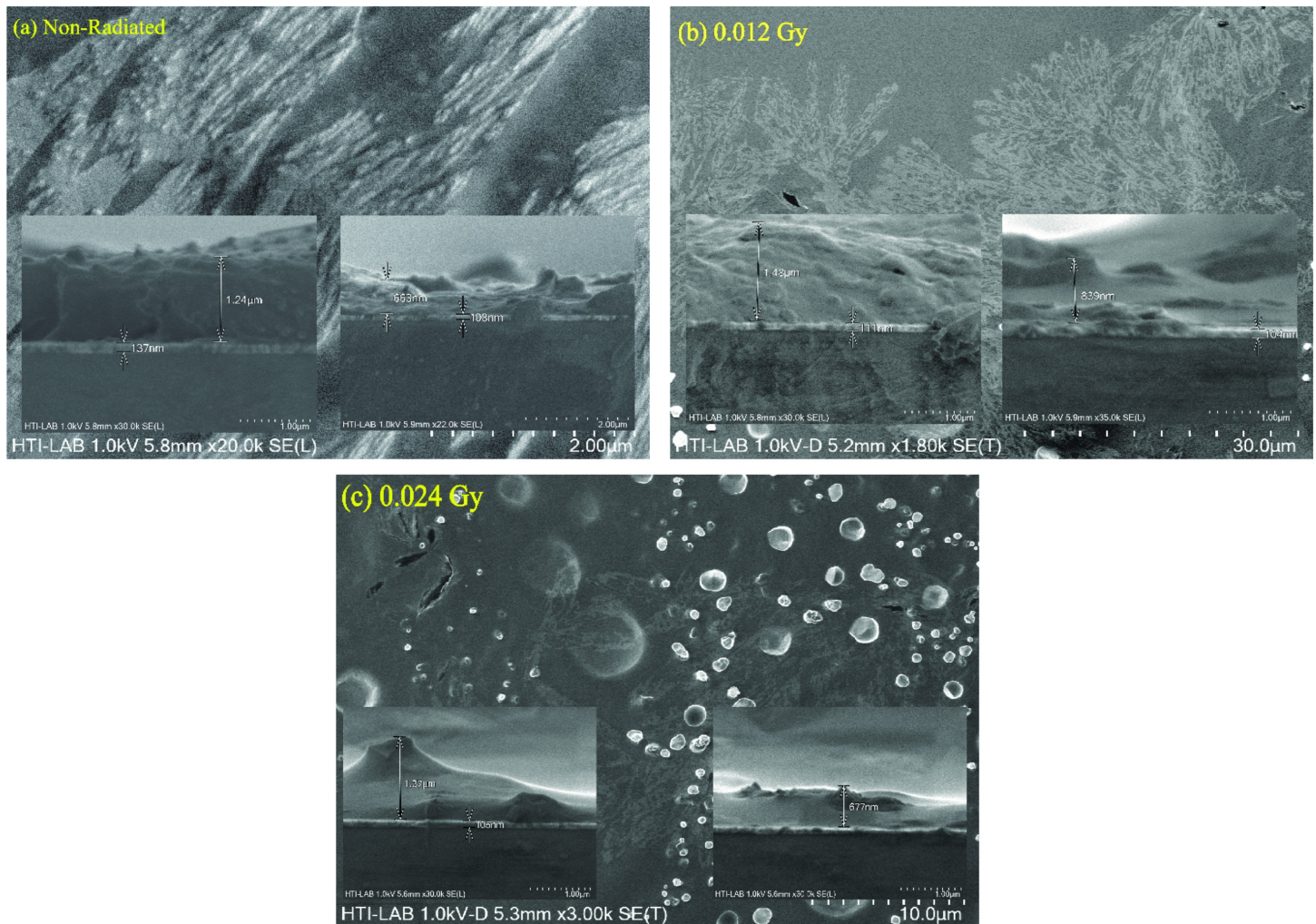


Fig 9. FESEM images of radiated and non-radiated samples.

doi:10.1371/journal.pone.0145423.g009

Space-charge-limited current (SCLC) effects the diode and its charge transport can be displayed through the $I = V^m$ rule where m is the slope of each part, which harmonize to ohmic and SCLC. The m values shown in Table 3 portray three linear parts of the $\log(I) - \log(V)$ plot of the forward bias I-V characterization. Part (I) shows an ohmic part, while the second part (II) demonstrates the presence of the SCLC mechanism controlled by the traps. The second part of this graph has slope values of between 1.9–4.8 up to a transition voltage of about ≈ 2.7 V, similar to the SCLC with the exponential distribution of traps in the band gap of the organic material. The third part of the double logarithmic forward bias curve has slope values of between 1.7–4.19 except for the sample with 0.24 Gy of radiation. This part shows that at higher voltages, the slope of the curve declines since the device approaches the trap filled limit.

The photoluminescence (PL) spectra of irradiated DNA were obtained. A red shift occurs at a range of 610 to 750 nm higher than the green wavelength (500–570 nm) due to the irradiation effect. The intensity of these peaks increases with an increase in the radiation dose. Luminescence phenomena involve subsequent light emission and energy absorption. Phosphors are luminescent materials that produce light after excitation by radiation, thin films or micro-crystalline powders, which usually produce visible color emission. This confirms that the purified

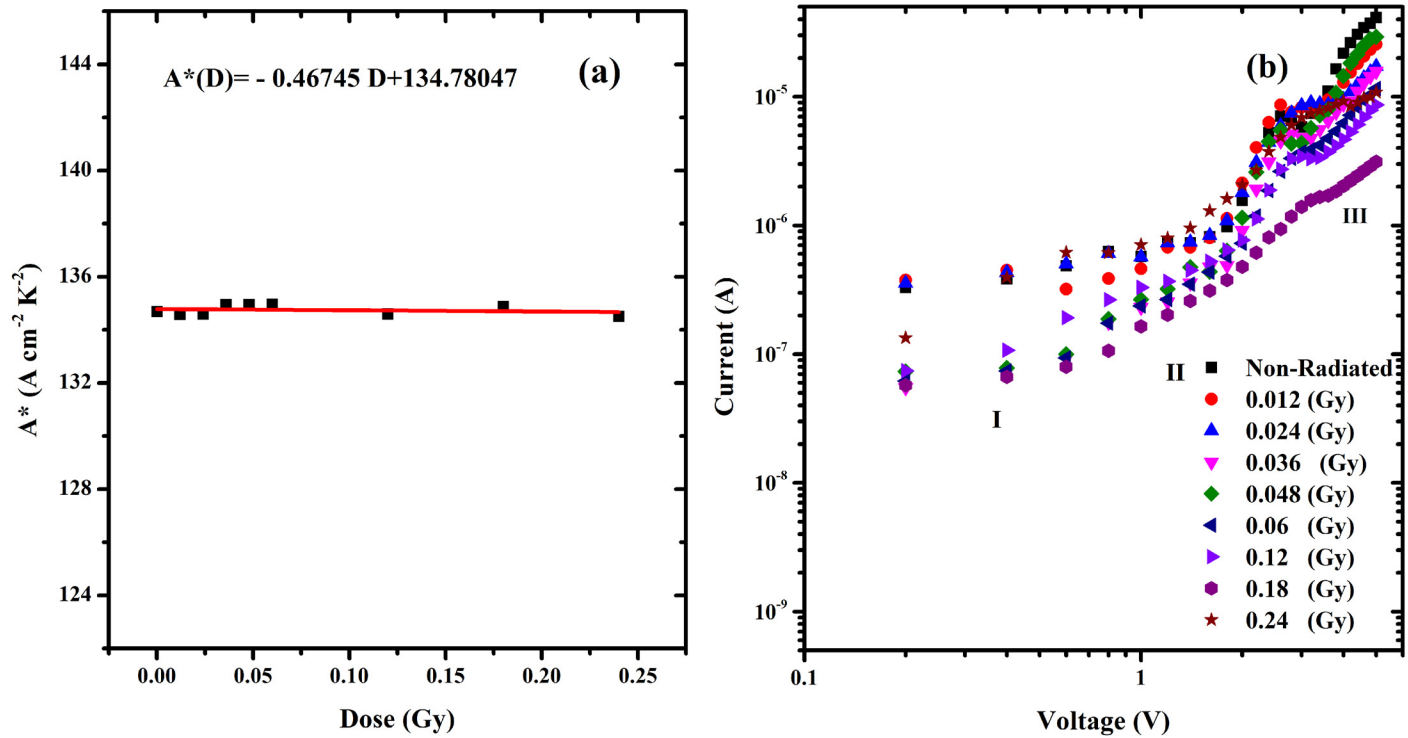


Fig 10. (a) Irradiation time dependent Richardson constant for the MDM structure and (b) double logarithmic plots of the ITO/DNA/Au junctions.

doi:10.1371/journal.pone.0145423.g010

DNA has a five-component linear triple complex involves of green, orange and red dots in the prepared. According to Tikhomirov *et al*, the complex exhibits pure red luminescence and is substantially devoid of the green and orange luminescence that was present before hybridization, and the linear ternary complex after cleavage by DNase, displaying the reversibility of complexation [51]. It is known that the emission spectrum of the nucleic acid bases (adenine, guanine, cytosine, thymine, uracil) is in the range of 400–600 nm, which indicates that the major contribution to the DNA PL spectrum are caused by these bases [48]. The homogeneous

Table 2. Barrier height and Richardson constant (A^*) against irradiation time in ITO/DNA/Au (ϕ) structures.

Dose (Gy)	Richardson constant	Barrier Height
	A^* ($\text{A.cm}^{-2}.\text{K}^{-2}$)	Φ (eV)
Non -Radiation	134.69052	0.7284
0.012	134.57489	0.7603
0.024	134.59185	0.7374
0.036	134.94212	0.7883
0.048	134.94788	0.7426
0.06	134.95653	0.7798
0.12	134.5969	0.7491
0.18	134.88262	0.7407
0.24	134.50431	0.7670

A^* ($\text{A.cm}^{-2}.\text{K}^{-2}$) = Richardson constant, Φ (eV) = Barrier Height.

doi:10.1371/journal.pone.0145423.t002

Table 3. Values of (m) for parts (I), (II) and (III) of the power law ITO/DNA/Au.

Dose (Gy)	ITO/DNA/Au Junction		
	(slope gradient,m)		
	Region (I)	Region (II)	Region (III)
Non -Radiation	0.45039	4.8048	4.19712
0.012	0.04507	3.552	2.8509
0.024	0.33099	3.63131	2.16649
0.036	0.88686	3.79171	2.69853
0.048	0.78422	3.26422	3.99268
0.06	0.8245	2.6816	2.37995
0.12	0.95396	2.49081	2.73198
0.18	0.41336	1.92962	1.73113
0.24	1.41163	2.16874	0.84589

doi:10.1371/journal.pone.0145423.t003

and specific bindings to DNA against intercalation between base-pairs and binding on phosphate backbones lead to the enhancing of the intensity of the PL [52].

Generally excitation and emission are considered significant processes in phosphors luminescence. Different types of energy could excite the phosphors, such as photon (often ultra-violet) that acts to excite the PL, an electric voltage to excite electroluminescence (EL) or

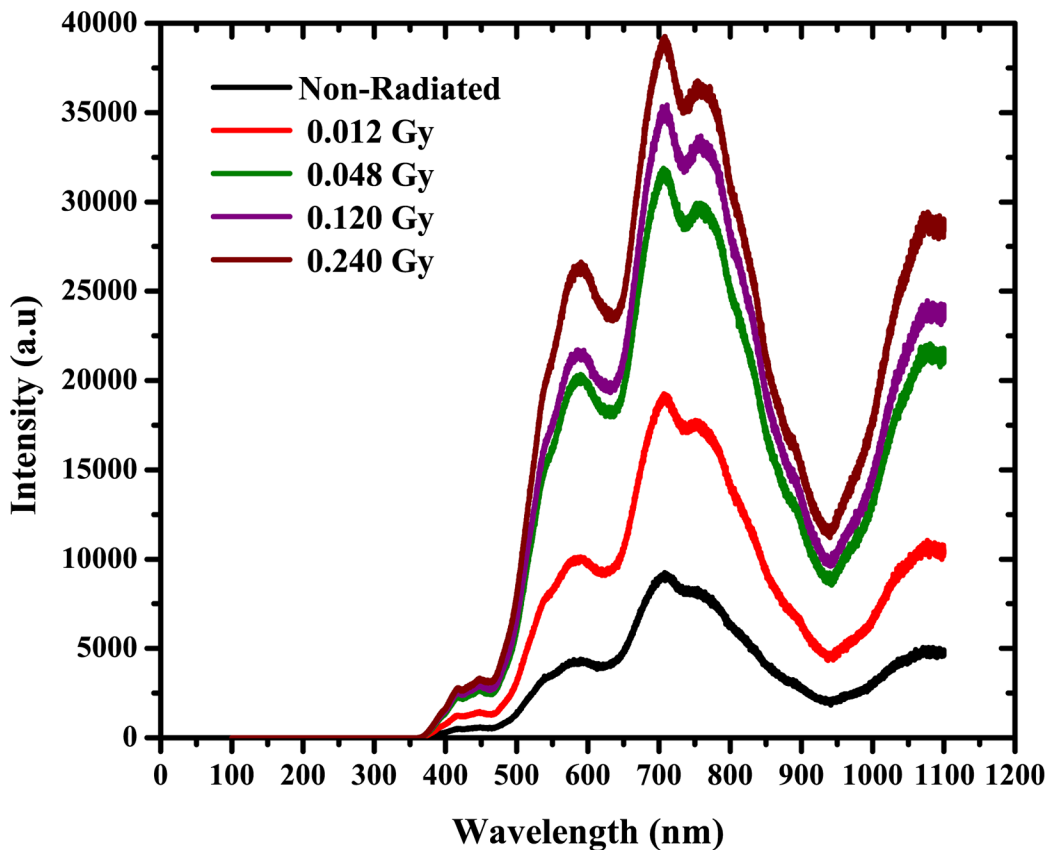


Fig 11. Photoluminescence spectra of DNA irradiated by alpha particles.

doi:10.1371/journal.pone.0145423.g011

chemiluminescence excited by the energy of a chemical reaction, and so on. The process of emission is a release of energy in the form of photon [53]. Therefore, the results demonstrated in this current work may suggest utilization as light emitting structures based on DNA diodes show Fig 11.

Conclusions

In this study, we fabricated surface-type ITO/DNA/Au Schottky barrier diodes and carried-out I-V measurements at room temperature. The electronic parameters such as the ideality factor, height barrier, series resistance and Richardson constant of the diode were also measured. In summary, we studied I-V characteristics of ITO/DNA/Au junctions exposed to different dosage (0–0.24 Gy). The metal-semiconductor-metal devices fabricated in this work demonstrated non-ideal I–V behavior. Barrier height determined from the I–V measurements were calculated at 0.7284 eV for non-radiation, increasing to about 0.7883 eV in 0.036 Gy of radiation, showing an increase for all doses. The radiation-induced hypersensitivity phenomena of the DNA used can be attributed to the changes observed in the ideality factors and series resistance values. It is therefore possible to utilize such fluctuations in Au/DNA/ITO junctions to enable rapid and accurate sensing or detection of alpha particles, also can be utilizing these devices as light emitting.

Acknowledgments

Financial assistances provided by Fundamental Research Grant Scheme, FRGS (FP004-2013A), University of Malaya Research Grant, UMRG (RG321-15AFR) and University of Malaya Postgraduate Research Fund, PPP (PG202-2014B) grant are greatly appreciated. The first author would also like to thank the Ministry of Higher Education and Scientific Research of Iraq for financial assistance provided for his PhD study.

Author Contributions

Conceived and designed the experiments: HMJA-T VP. Performed the experiments: HMJA-T. Analyzed the data: HMJA-T VP. Contributed reagents/materials/analysis tools: VP HMJA-T YMA. Wrote the paper: HMJA-T VP.

References

1. Güllü Ö, Cankaya M, Barış Ö, Türüt A. DNA-modified indium phosphide Schottky device. *Appl Phys Lett*. 2008; 92(21):212106.
2. Sönmezoğlu S, Ateş Sönmezoğlu Ö. Optical and dielectric properties of double helix DNA thin films. *Materials Science and Engineering: C*. 2011; 31(8):1619–24. <http://dx.doi.org/10.1016/j.msec.2011.08.003>.
3. Güllü Ö, Çankaya M, Barış Ö, Biber M, Özdemir H, Güllüce M, et al. DNA-based organic-on-inorganic semiconductor Schottky structures. *Appl Surf Sci*. 2008; 254(16):5175–80. <http://dx.doi.org/10.1016/j.apsusc.2008.02.019>.
4. Batcup S, Wills J, Lodzinski M, Wright C, Doak S, Holland P, et al. Modification of Schottky interface by the inclusion of DNA interlayer to create metal/organic/inorganic structures. *Microelectronics (MIEL)*, 2012 28th International Conference on: IEEE; 2012. p. 81–4.
5. Lu J, Yang L, Xie A, Shen Y. DNA-templated photo-induced silver nanowires: fabrication and use in detection of relative humidity. *Biophys Chem*. 2009; 145(2):91–7.
6. Khatir NM, Banihashemian SM, Periasamy V, Ritikos R, Majid WHA, Rahman SA. Electrical characterization of Gold-DNA-Gold structures in presence of an external magnetic field by means of I-V curve analysis. *Sensors*. 2012; 12(3):3578–86. doi: [10.3390/s120303578](https://doi.org/10.3390/s120303578) PMID: [22737025](https://pubmed.ncbi.nlm.nih.gov/22737025/)
7. Banihashemian S, Periasamy V, Mohammadi S, Ritikos R, Rahman S. Optical Characterization of Oligonucleotide DNA Influenced by Magnetic Fields. *Molecules*. 2013; 18(10):11797–808. doi: [10.3390/molecules181011797](https://doi.org/10.3390/molecules181011797) PMID: [24071986](https://pubmed.ncbi.nlm.nih.gov/24071986/)

8. Güllü Ö, Türüt A. Electronic properties of Al/DNA/p-Si MIS diode: Application as temperature sensor. *Journal of Alloys and Compounds*. 2011; 509(3):571–7. <http://dx.doi.org/10.1016/j.jallcom.2010.09.146>.
9. Kulkarni A, Kim B, Dugasani SR, Joshirao P, Kim JA, Vyas C, et al. A novel nanometric DNA thin film as a sensor for alpha radiation. *Scientific report*. 2013; 3.
10. Al-Ta'ii HMJ, Amin YM, Periasamy V. Investigations of electrical properties of structures Al-DNA-ITO-Al exposed to alpha particles. *Radiation Measurements*. 2015; 72:85–94.
11. Bonea A, Rau I, Tane A, Svasta P. Effects of temperature and humidity on DNA-based biopolymers. *Journal of Optoelectronics and Advanced Materials*. 2012; 14(5–6):511–6.
12. Takada T, Fujitsuka M, Majima T. Single-molecule observation of DNA charge transfer. *Proceedings of the National Academy of Sciences*. 2007; 104(27):11179–83.
13. Tsoulou E, Kalfas C, Sideris E. Changes in DNA flexibility after irradiation with γ rays and neutrons studied with the perturbed angular correlation method. *Radiation research*. 2003; 159(1):33–9. PMID: [12492366](https://pubmed.ncbi.nlm.nih.gov/12492366/)
14. Ş. Aydoğan ÖG, Türüt A. Fabrication an electrical properties of Al /aniline green/n-Si/Au Sbstructure. *Materials Science in Semiconductor Processing*. 2008; 11:53–8.
15. Bazlov NV, Vyvenko OF, Sokolov PA, Kas'yanenko NA, Petrov YV. Charge-controlled fixation of DNA molecules on silicon surface and electro-physical properties of Au–DNA–Si interface. *Appl Surf Sci*. 2013; 267(0):224–8. <http://dx.doi.org/10.1016/j.apsusc.2012.11.002>.
16. Jo Y-S, Lee Y, Roh Y. Effects of humidity on the electrical conduction of lambda-DNA trapped on a nano-gap Au electrode. *Journal of the Korean Physical Society*. 2003; 43(2):909–13.
17. Otsuka Y, Lee H-y, Gu J-h, Lee J-O, Yoo K-H, Tanaka H, et al. Influence of humidity on the electrical conductivity of synthesized DNA film on nanogap electrode. *Japanese journal of applied physics*. 2002; 41(2R):891.
18. Jayavel P, Kumar J, Santhakumar K, Magudapathy P, Nair K. Investigations on the effect of alpha particle irradiation-induced defects near Pd/n-GaAs interface. *Vacuum*. 2000; 57(1):51–9.
19. Al-Ta'ii HMJ, Amin YM, Periasamy V. Calculation of the Electronic Parameters of an Al/DNA/p-Si Schottky Barrier Diode Influenced by Alpha Radiation. *Sensors*. 2015; 15(3):4810–22. doi: [10.3390/s150304810](https://doi.org/10.3390/s150304810) PMID: [25730484](https://pubmed.ncbi.nlm.nih.gov/25730484/)
20. Holbert KE. *Radiation Effects Damage*2012.
21. Gupta RK, Yakuphanoglu F. Photoconductive Schottky diode based on Al/p-Si/SnS₂/Ag for optical sensor applications. *Solar Energy*. 2012; 86(5):1539–45. <http://dx.doi.org/10.1016/j.solener.2012.02.015>.
22. Sönmezoğlu S, Sönmezoğlu ÖA, Çankaya G, Yıldırım A, Serin N. Electrical characteristics of DNA-based metal-insulator-semiconductor structures. *Journal of Applied Physics*. 2010; 107(12):124518.
23. Bellido EP, Bobadilla AD, Rangel NL, Zhong H, Norton ML, Sinitskii A, et al. Current–voltage–temperature characteristics of DNA origami. *Nanotechnology*. 2009; 20(17):175102. doi: [10.1088/0957-4484/20/17/175102](https://doi.org/10.1088/0957-4484/20/17/175102) PMID: [19420582](https://pubmed.ncbi.nlm.nih.gov/19420582/)
24. Bixon M, Giese B, Wessely S, Langenbacher T, Michel-Beyerle ME, Jortner J. Long-range charge hopping in DNA. *Proceedings of the National Academy of Sciences*. 1999; 96(21):11713–6.
25. Ha DH, Nham H, Yoo K-H, So H-m, Lee H-Y, Kawai T. Humidity effects on the conductance of the assembly of DNA molecules. *Chemical physics letters*. 2002; 355(5):405–9.
26. Güllü Ö, Cankaya M, Barış Ö, Biber M, Özdemir H, Güllüce M, et al. DNA-based organic-on-inorganic semiconductor Schottky structures. *Appl Surf Sci*. 2008; 254(16):5175–80.
27. Heim T, Deresmes D, Vuillaume D. Conductivity of DNA probed by conducting–atomic force microscopy: Effects of contact electrode, DNA structure, and surface interactions. *Journal of Applied Physics*. 2004; 96(5):2927–36.
28. Okahata Y, Kobayashi T, Tanaka K, Shimomura M. Anisotropic electric conductivity in an aligned DNA cast film. *Journal of the American Chemical Society*. 1998; 120(24):6165–6.
29. Dugasani SR, Kim M, Lee I-y, Kim JA, Gnapareddy B, Lee KW, et al. Construction and characterization of Cu²⁺, Ni²⁺, Zn²⁺, and Co²⁺ modified-DNA crystals. *Nanotechnology*. 2015; 26(27):275604. doi: [10.1088/0957-4484/26/27/275604](https://doi.org/10.1088/0957-4484/26/27/275604) PMID: [26086080](https://pubmed.ncbi.nlm.nih.gov/26086080/)
30. Dugasani SR, Lee KW, Kim SJ, Yoo S, Gnapareddy B, Jung J, et al. Hall transport of divalent metal ion modified DNA lattices. *Applied Physics Letters*. 2015; 106(26):263702.
31. Hibbett D. Forensic DNA mini-prep using the E.Z.N.A. kit. 2013 [20 Oct.2013]. Available from: Available: <http://www.clarku.edu/faculty/dhibbett/protocols.htm>. Accessed 20 October 2013.
32. Intiaj A, Lee T, Ohga S. Sequence Variation of Pleurotus Species Collected From Eastern Asia. *Micol Aplicada Int*. 2011; 23(1).

33. Cubero OF, Crespo A, Fatehi J, Bridge PD. DNA extraction and PCR amplification method suitable for fresh, herbarium-stored, lichenized, and other fungi. *Plant Systematics and Evolution*. 1999; 216(3–4):243–9.
34. Tuğluoğlu N, Karadeniz S. Analysis of current–voltage and capacitance–voltage characteristics of perylene-monoimide/n-Si Schottky contacts. *Current Applied Physics*. 2012; 12(6):1529–35.
35. Kılıçoğlu T, Ocak YS. Electrical and photovoltaic properties of an organic–inorganic heterojunction based on a BODIPY dye. *MICROELECTRON ENG*. 2011; 88(2):150–4.
36. Karataş Ş, Türüt A. The determination of interface state energy distribution of the H-terminated Zn/p-type Si Schottky diodes with high series resistance by the admittance spectroscopy. *Vacuum*. 2004; 74(1):45–53.
37. Muhammad Tahir, Muhammd. H. Sayyad, Muhammad Shahid, Jamil. A. Chaudry, A. Munawar, editors. Fabrication of Al/N-BuHHPDI/ITO Schottky Barrier Diode and Investigation of its Electrical Properties. International Conference on Advances in Electrical and Electronics Engineering (ICAEEE'2012); 2012 April 13–15.
38. Güllü Ö, Pakma O, Türüt A. Current density-voltage analyses and interface characterization in Ag/DNA/p-InP structures. *Journal of Applied Physics*. 2012; 111(4):044503.
39. Mahmoudi Khatir N. Electrical characterization of metal-DNA-metal device under the influence of magnetic field: University of Malaya; 2013.
40. Okur S, Yakuphanoglu F, Ozsoz M, Kadayifcilar PK. Electrical and interface properties of Au/DNA/n-Si organic-on-inorganic structures. *MICROELECTRON ENG*. 2009; 86(11):2305–11. <http://dx.doi.org/10.1016/j.mee.2009.04.017>.
41. Reddy VS, Das K, Dhar A, Ray S. The effect of substrate temperature on the properties of ITO thin films for OLED applications. *Semiconductor science and technology*. 2006; 21(12):1747–52.
42. Cheung SKCaNW. Extraction of Schottky diode parameters from forward current-voltage characteristics.,. *Appl Phys Lett*. 1986; 49(2):p. 85–7.
43. Reddy M, Kim B-J, Jang J-S. Dual detection of ultraviolet and visible lights using a DNA-CTMA/GaN photodiode with electrically different polarity. *Optics express*. 2014; 22(1):908–15. doi: [10.1364/OE.22.000908](https://doi.org/10.1364/OE.22.000908) PMID: [24515050](https://pubmed.ncbi.nlm.nih.gov/24515050/)
44. Schmitsdorf R, Kampen T, Monch W. Explanation of the linear correlation between barrier heights and ideality factors of real metal-semiconductor contacts by laterally nonuniform Schottky barriers. *Journal of Vacuum Science & Technology B: Microelectronics and Nanometer Structures*. 1997; 15(4):1221–6.
45. Norde H. A modified forward I-V plot for Schottky diodes with high series resistance. *Journal of Applied Physics*. 2008; 50(7):5052–3.
46. Martin LM, Marples B, Lynch TH, Hollywood D, Marignol L. Exposure to low dose ionising radiation: Molecular and clinical consequences. *Cancer letters*. 2013; 338(2):209–18. doi: [10.1016/j.canlet.2013.05.021](https://doi.org/10.1016/j.canlet.2013.05.021) PMID: [23693079](https://pubmed.ncbi.nlm.nih.gov/23693079/)
47. Hassan M. Al-Tai'i and MAASa. hypersensitivity phenomenon in hydatid protoscolices irradiated by alpha particles. *Jouenal of Kerbala University*. 2012; 10(1):41–4.
48. Hassan M. Al-Tai'i A, Khalid D, Azooz Faika. A. Observation of Hypersensitivity Phenomena in E-Coli Cells after Irradiation by Alpha Particles. *Journal Rafiden Science*. 2009; 20:113–20.
49. Sabet M, Hassan A, Ratnam C. Mechanical, electrical, and thermal properties of irradiated low-density polyethylene by electron beam. *Polym Bull*. 2012; 68(9):2323–39. doi: [10.1007/s00289-012-0741-y](https://doi.org/10.1007/s00289-012-0741-y)
50. Ziaie F, Bolorizadeh MA. Electrical properties of EVA/LDPE blends irradiated by high energy electron beam. *Nukleonika*. 2007; 52(2):77–81.
51. Tikhomirov G, Hoogland S, Lee P, Fischer A, Sargent EH, Kelley SO. DNA-based programming of quantum dot valency, self-assembly and luminescence. *Nature nanotechnology*. 2011; 6(8):485–90. doi: [10.1038/nnano.2011.100](https://doi.org/10.1038/nnano.2011.100) PMID: [21743454](https://pubmed.ncbi.nlm.nih.gov/21743454/)
52. Dugasani SR, Park B, Gnapareddy B, Pamanji SR, Yoo S, Lee KW, et al. Tunable near white light photoluminescence of lanthanide ion (Dy 3+, Eu 3+ and Tb 3+) doped DNA lattices. *RSC Advances*. 2015; 5(69):55839–46.
53. Shinde KN, Dhoble S, Swart H, Park K. Basic Mechanisms of Photoluminescence. *Phosphate Phosphors for Solid-State Lighting*: Springer; 2012. p. 41–59.